

# Synthesis, Characterization, and Catalytic Activity of NAPO-5 and NAPO-11

Shanmugam P. Elangovan, Vengaimuthu Krishnasamy, and Velayutham Murugesan\*

Department of Chemistry, Anna University, Madras-600025, India

(Received March 31, 1995)

Nickel-substituted aluminophosphate molecular sieves (NAPO-5 and NAPO-11) were synthesized hydrothermally using triethylamine and dipropylamine as templates. Structures were confirmed by X-ray powder pattern, and unit cell parameters calculated by a standard least square refinement technique. The isomorphous substitution of nickel in the aluminophosphate framework is evidenced by the considerable increase in unit cell volume compared to unsubstituted  $\text{AlPO}_4$ -5 and  $\text{AlPO}_4$ -11. In addition, electron spin resonance and diffuse reflectance spectra were carried out to produce supporting evidence for the isomorphous substitution of nickel. Acidity was determined by a TPD-TGA method which shows two types of acid sites. Symmetry and asymmetry vibrations were obtained from infrared spectra. Chemical analysis by ICP and BET surface area are also reported. The physicochemical properties of the catalysts were correlated towards isomerisation of camphene at various  $(\text{WHSV})^{-1}$  values and temperatures. The products formed are tricyclene and 2-bornene and the selective formation of tricyclene was achieved over these catalysts.

The recent break-through in zeolite chemistry has initiated interest in the synthesis and investigation of new types of zeolite-like materials. Among them crystalline aluminophosphates, silicoaluminophosphates, and metal aluminophosphates are the most interesting and promising from the point of view of their applications in catalysis.<sup>1)</sup> The introduction of Brønsted acidity in aluminophosphate molecular sieves requires isomorphous substitution of lower valency elements for  $\text{Al}^{3+}$  or  $\text{P}^{5+}$  in  $[\text{AlO}_2]^-$  and  $[\text{PO}_2]^+$  building units of the  $\text{AlPO}_4$  framework. Metal substituted aluminophosphates (MeAPO) mark the first demonstrated incorporation of divalent forms of cobalt, iron, magnesium, manganese, and zinc into a microporous framework during synthesis.<sup>2,3)</sup> The preferred substitution in MeAPO is via the mechanism proposed by Flanigen et al.,<sup>4)</sup> wherein the metal ion isomorphously replaces an aluminium from the  $\text{AlPO}_4$  framework. Substitution of divalent nickel into silicoaluminophosphate framework has been reported by Inui et al., who studied the selective synthesis of ethene from methanol.<sup>5)</sup> Among the known aluminophosphate molecular sieves,  $\text{AlPO}_4$ -5 and  $\text{AlPO}_4$ -11 have gained considerable attention on account of their straight channel system.

In the present study, nickel samples containing  $\text{AlPO}_4$ -5 and  $\text{AlPO}_4$ -11 were synthesised. Their structure, surface properties, and acidity were investigated by means of XRD, IR, DRS, ESR, BET surface area, chemical analysis, and TPD of pyridine; their catalytic activity towards isomerisation of camphene was also carried out.

## Experimental

**Materials.** Aluminium isopropoxide (Fluka), nickel acetate (BDH), orthophosphoric acid (85% Qualigens), triethylamine (TEA) (Fluka), dipropylamine (DPA) (Fluka), and camphene (Fluka) were used as purchased.

**Synthesis of NAPO-5.** NAPO-5 was synthesized using the following gel composition: 0.1 NiO : 1 TEA : 1  $\text{Al}_2\text{O}_3$  : 1  $\text{P}_2\text{O}_5$  : 40  $\text{H}_2\text{O}$ . Aluminium isopropoxide (28.37 g) in 30 ml distilled water was soaked for a day. On the day of the synthesis, it was placed in an autoclave and vigorously stirred for 1 h. Phosphoric acid (7.8 ml) diluted with 10 ml distilled water was mixed with 1.73 g nickel(II) acetate in 10 ml distilled water. The clear green solution was added dropwise to the autoclave (300 ml, 316 type) and stirred for 1 h. TEA (9.7 ml) was added slowly and further stirred for 1 h. The gel pH was 4.9. The autoclave was kept under autogenous pressure at 175 °C for 22 h. The autoclave was cooled to room temperature to get the final product, whose pH was 9.0. The product was washed with water several times and dried at 110 °C for 12 h.

**Synthesis of NAPO-11.** Homogeneous gel composition of 0.1 NiO : 1 DPA : 1  $\text{Al}_2\text{O}_3$  : 1  $\text{P}_2\text{O}_5$  : 40  $\text{H}_2\text{O}$  was used for the synthesis of NAPO-11. Aluminium isopropoxide (28.37 g) was soaked in 30 ml distilled water for 24 h and then stirred vigorously for 1 h. Nickel acetate (1.73 g) was dissolved in 10 ml distilled water and then mixed with 7.8 ml phosphoric acid diluted with 10 ml distilled water. The clear green solution was added dropwise to the above contents with constant stirring. The slurry was stirred for 1 h, DPA (9.5 ml) was added slowly and the stirring continued for another 1 h. pH of the gel was 4.0. The resultant gel was placed in a stainless steel autoclave under autogenous pressure at 200 °C for 22 h. The pH of the final product

was 9.1. The product was washed with distilled water and dried at 110 °C for 12 h.

Half of the each sample was calcined at 550 °C for 8 h to remove the template present in the sample.

**Characterization.** X-Ray diffraction analysis was carried out in a Siemens D500 diffractometer in the scan range of  $2\theta$  between 5 and 50° using Cu  $K\alpha$  as source. The peaks were identified with reference to compilation of simulated XRD powder pattern.<sup>6)</sup> Unit cell parameters were calculated using a standard least square refinement technique. ESR analysis was carried out using a Varian E112 spectrophotometer at room temperature. Diffuse reflectance spectra (DRS) were recorded in the wave length range 300–800 nm using a Cary 2390 UV-vis-NIR spectrophotometer. IR spectra of the samples were recorded on a Bruker IFS 66v FT-IR spectrophotometer using KBr pellet. TGA of the samples were carried out with a Mettler TA 3000 system at a scanning rate of 20 °C min<sup>-1</sup> in a stream of dry air. Inductively Coupled Plasma (ICP) ARL 3410 with a minitorch was used to find the chemical composition of the samples. Surface area measurements were carried out in a Micromeritics Pulse Chemisorb 2700 using nitrogen as adsorbent at -176 °C. Initially the samples were degasified at 200 °C for 2 h in a flow of oxygen.

**Acidity.** Acidity of the samples was measured by Temperature Programmed Desorption (TPD) of pyridine using TGA (Mettler TA 3000 system). Prior to adsorption, the samples were evacuated to 10<sup>-3</sup> Torr (1 Torr=133.322 Pa) at 450 °C for 2 to 3 h. Then pyridine in a closed vessel was allowed to equilibrate at room temperature. TG analysis was carried out up to 500 °C at a scanning rate of 10 °C min<sup>-1</sup>. From the weight loss at various temperature ranges, acidity and acidic strength in mmol g<sup>-1</sup> were determined.

**Catalytic Studies.** The reactor system was a fixed-bed, vertical, flow type reactor made up of a quartz tube of 40 cm length and 2 cm internal diameter. The quartz reactor was heated to the requisite temperature with the help of a tubular furnace controlled by a digital temperature controller cum indicator. The bottom of the reactor was provided with a thermowell in which the chromel–alumel thermocouple was kept to measure the temperature at the middle of the catalyst bed. About 2 g of the catalyst (20–

40 mesh size) was taken in the reactor and supported on either side with a thin layer of quartz wool and ceramic beads. The top portion of the reactor was connected to a glass bulb having two inlets. Reactant was fed into the reactor through one inlet by a syringe infusion pump that can be operated at different flow rates. The bottom of the reactor was connected to a coiled condenser and a receiver in which the products were collected.

The liquid products collected for the first 15 min of each run were discarded and analysis was made only for the products collected after this time. This was done to ensure the attainment of steady state for the reaction and also to allow any temperature fluctuation to stabilize. After each catalytic run, the catalyst was regenerated by passing air free from carbon dioxide through the reactor at 500 °C for 6 h. The liquid products were analyzed by a Hewlett Packard gas chromatograph 5890 A using a flame ionisation detector with carbowax as column and nitrogen as carrier gas. Injector temperature, detector temperature, and oven temperature were 160, 225, and 110–180 °C, respectively.

## Results and Discussion

**Structure.** XRD patterns of as-synthesised NAPO-5 and NAPO-11 are shown in Figs. 1 and 2 respectively. The patterns are well-matched with the reported patterns.<sup>6)</sup> Unit cell parameters were calculated for both as-synthesised and calcined samples and are listed in Table 1. They are compared with unit cell parameters of AlPO<sub>4</sub>-5 and AlPO<sub>4</sub>-11 synthesised using the templates TEA and DPA respectively.<sup>7–9)</sup> Substitution of nickel for aluminium considerably increases the overall unit cell volume which is a convincing piece of evidence for the isomorphous substitution of Ni<sup>2+</sup> in the aluminophosphate framework. However, the decrease in unit cell volume for the calcined samples may be attributed to the removal of strain after the loss of templates from the voids. The incorporation of nickel into the aluminophosphate framework may also be evident from the ESR spectra, which exhibits two transitions with parameters  $g_{\parallel}$  2.09 and  $g_{\perp}$  2.07 for NAPO-5

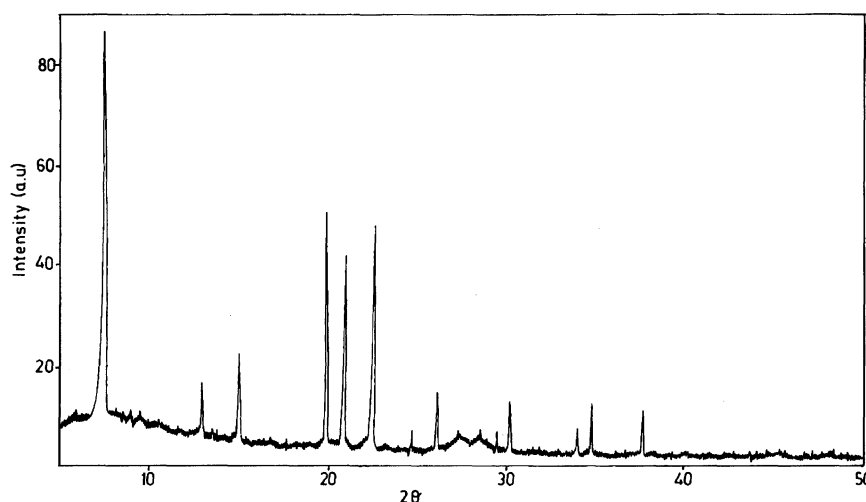


Fig. 1. XRD pattern of NAPO-5.

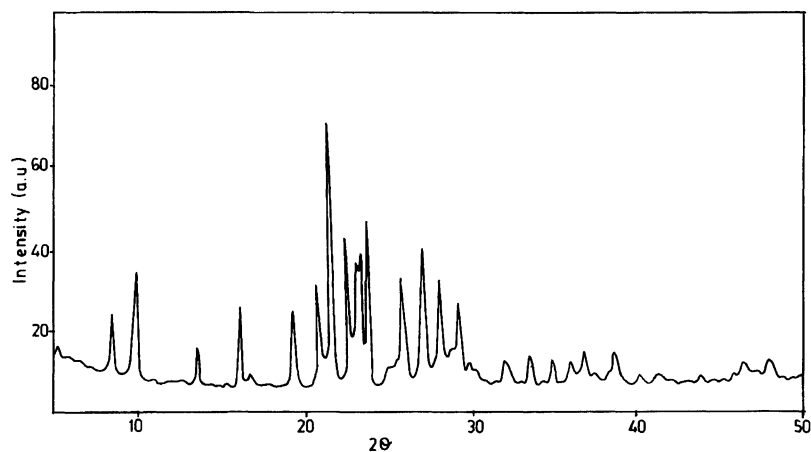


Fig. 2. XRD pattern of NAPO-11.

Table 1. Unit Cell Parameters and Unit Cell Volume

Catalyst	$a/\text{Å}$	$b/\text{Å}$	$c/\text{Å}$	$v/\text{Å}^3$
As-synthesised				
NAPO-5	13.74	13.74	8.47	1385
NAPO-11	13.50	18.62	8.43	2114
Calcined				
NAPO-5	13.67	13.67	8.48	1372
NAPO-11	13.71	18.55	8.21	2088
AlPO <sub>4</sub> -5	13.64	13.64	8.49	1368 (Ref. 7–9)
AlPO <sub>4</sub> -11	13.48	18.56	8.39	2099 (Ref. 7–9)

and  $g_{\parallel}$  2.08 and  $g_{\perp}$  2.07 for NAPO-11. The absorption bands in wavelength range 550–800 nm in the diffuse reflectance spectra are the supporting evidence for the presence of nickel in the aluminophosphate framework. FT-IR spectra of as-synthesised NAPO-5 and NAPO-

11 in the region encompassing the framework vibrations and -OH vibration are depicted in Fig. 3.

TG and their corresponding derivative curves (DTG) of the samples are shown in Fig. 4. These samples show a low temperature weight loss around 100 °C which is attributed to the loss of water and also high temperature weight losses in the temperature range 250–550 °C which are ascribed to the desorption of templates present in the intracrystalline pores. The desorption of templates proceeds in multiple stages, possibly the release of template first as free amine at a low temperature and then by degradation of proton or metal complexed amine at high temperature.<sup>10)</sup> The total weight loss is about 13.7 and 9.5% for NAPO-5 and NAPO-11 respectively.

Chemical analysis gave the compositions corresponding to NiO:Al<sub>2</sub>O<sub>3</sub>:P<sub>2</sub>O<sub>5</sub> as 0.05:0.96:1 and 0.04:0.97:1 for NAPO-5 and NAPO-11 respectively. This indicates that nickel replaces aluminium in the

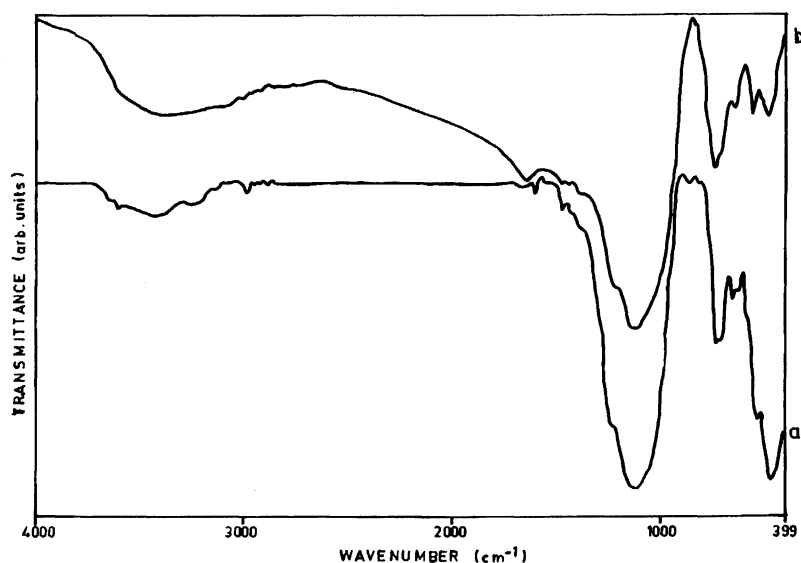


Fig. 3. FT-IR spectra of NAPO-5 (a) and NAPO-11 (b).

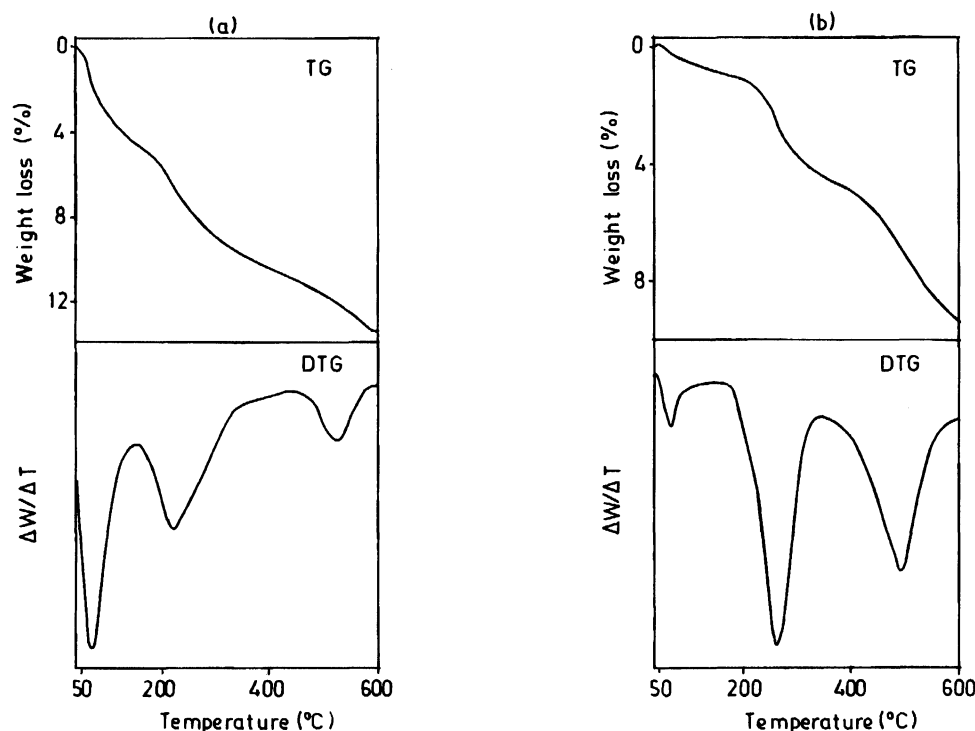


Fig. 4. TG and DTG curves of NAPO-5 (a) and NAPO-11 (b).

framework. The extent of nickel substitution in the framework is only about 50% and moreover, the substitution is higher for NAPO-5 than NAPO-11. BET surface area of the catalysts are presented in Table 2 where NAPO-5 possesses higher surface area than NAPO-11 due to large pore size. However the surface areas of NAPO-5 and NAPO-11 are almost similar to those of  $\text{AlPO}_4\text{-5}$  ( $221 \text{ m}^2 \text{ g}^{-1}$ ) and  $\text{AlPO}_4\text{-11}$  ( $204 \text{ m}^2 \text{ g}^{-1}$ ). This demonstrates that the incorporation of nickel is not blocking the pores of the structure.<sup>11)</sup>

**Acidity.** The acid amount of the catalysts was determined by TPD from pyridine desorption. The values are given in Table 2. The weight losses at two different temperature ranges, viz., 130–190 °C and 190–280 °C, are the indication of the presence of acid sites in two different strengths. The weight loss in the temperature range 40–130 °C is due to the loss of physisorbed pyridine. The higher acidity value of NAPO-5 may be due to more nickel substitution in NAPO-5 than in NAPO-11; this has been evidenced from chemical analysis studies.

**Camphene Isomerization.** Camphene was well-known as a transformation product of  $\alpha$ -pinene long

before it was found in nature. Its isomerization product tricyclene is used as a fragrant chemical as well as a good solvents.<sup>12,13)</sup> In the present study, isomerization of camphene over NAPO-5 and NAPO-11 was carried out. The transformation products are mainly tricyclene and 2-bornene.

**Effect of  $(\text{WHSV})^{-1}$ .** The effect of  $(\text{WHSV})^{-1}$  on the conversion of camphene, products yield, and products selectivity over NAPO-5 and NAPO-11 is presented in Table 3. The data presented in the Table illustrate that an increase in  $(\text{WHSV})^{-1}$  increases the overall conversion of camphene and product yields. However, selectivity of tricyclene decreases with increase in

Table 3. Effect of  $(\text{WHSV})^{-1}$  on the Camphene Conversion and Product Distribution

Sample	Temperature=300 °C			
	Time on stream=1 h			
	$(\text{WHSV})^{-1}/\text{h}$			
	0.4	0.8	1.2	1.6
<b>NAPO-5</b>				
Camphene conversion (wt%)	30.6	38.2	45.3	51.6
Tricyclene yield (wt%)	26.8	31.9	35.4	37.4
2-Bornene yield (wt%)	3.8	6.3	9.9	14.2
Tricyclene selectivity (%)	87.7	83.5	78.1	72.4
2-Bornene selectivity (%)	12.3	16.5	21.9	27.6
<b>NAPO-11</b>				
Camphene conversion (wt%)	22.8	28.3	32.7	37.5
Tricyclene yield (wt%)	20.4	24.3	26.8	29.0
2-Bornene yield (wt%)	2.4	4.0	5.9	8.5
Tricyclene selectivity (%)	89.3	85.8	81.9	77.3
2-Bornene selectivity (%)	10.7	14.2	18.1	22.7

Table 2. Acidity and Surface Area of NAPO-5 and NAPO-11

Catalyst	Desorption of pyridine		Total acid amount	BET surface area
	130–190 °C	190–280 °C		
	$\text{mmol g}^{-1}$		$\text{mmol g}^{-1}$	$\text{m}^2 \text{ g}^{-1}$
NAPO-5	0.16	0.14	0.30	233
NAPO-11	0.14	0.12	0.26	199

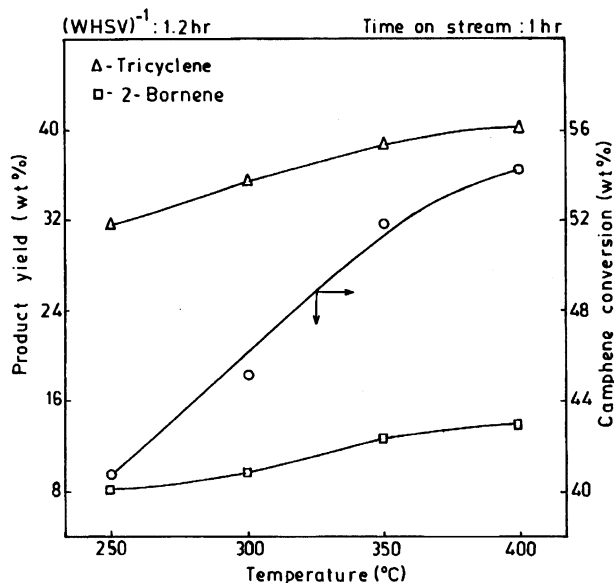


Fig. 5. Effect of temperature on camphene conversion and products yield over NAPO-5.

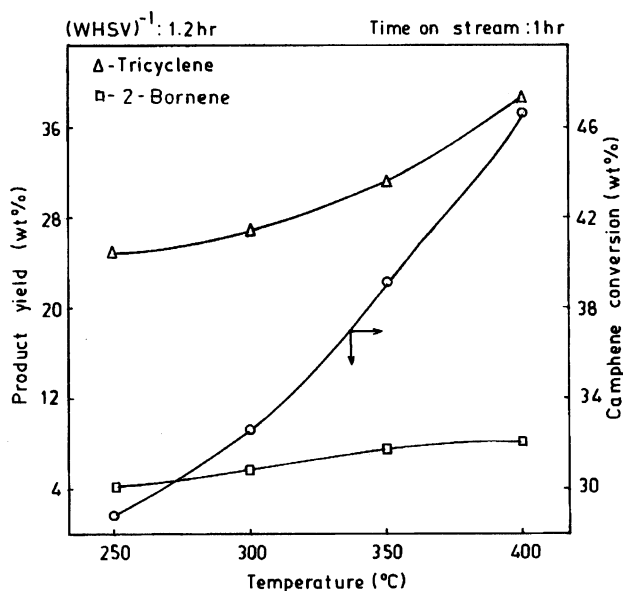


Fig. 6. Effect of temperature on camphene conversion and products yield over NAPO-11.

(WHSV)<sup>-1</sup>. These results indicate that selective formation of tricyclene is favorable at lower (WHSV)<sup>-1</sup>, whereas the formation of 2-bornene is found at higher (WHSV)<sup>-1</sup>.

**Effect of Temperature.** The effects of temperature on camphene conversion and products yield over the catalysts are represented in Figs. 5 and 6. Though at a given temperature the actual conversion is dif-

ferent for the two catalysts, as temperature increases from 250–450 °C, the camphene conversion and product yield increase with respect to both catalysts.

**Influence of Acidity.** Acidity has a direct bearing on camphene conversion. For instance, the conversion of camphene over NAPO-11 at 350 °C and 1.2 h (WHSV)<sup>-1</sup> is 39.2%, whereas under the same conditions the conversion is 51.9% over NAPO-5, due to the difference in acidity values (Table 2). Further, increase in acidity decreases the selectivity of tricyclene, whereas 2-bornene selectivity increases.

### Conclusion

Strict alternation of [AlO<sub>2</sub>]<sup>-</sup> and [PO<sub>2</sub>]<sup>+</sup> tetrahedra made aluminophosphate molecular sieves become neutral framework. Isomorphous substitution of divalent nickel over AlPO<sub>4</sub>-5 and AlPO<sub>4</sub>-11 may be successful and thereby change their physicochemical and catalytic properties. Further, we conclude that weak acid sites and lower (WHSV)<sup>-1</sup> are sufficient conditions for the selective formation of tricyclene.

### References

- 1) E. M. Flanigen, B. M. Lok, R. L. Patton, and S. T. Wilson, "New Developments in Zeolite Science and Technology," ed by Y. Murakami et al., Elsevier, Amsterdam (1986), p. 103.
- 2) S. T. Wilson and E. M. Flanigen, U. S. Patent 4567029 (1986).
- 3) R. R. Malherbe, R. L. Cordero, J. A. G. Morales, J. O. Martinez, and M. C. Gracial, *Zeolites*, **13**, 481 (1993).
- 4) E. M. Flanigen, R. L. Patton, and S. T. Wilson, "Innovation in Zeolite Materials Science," ed by P. J. Grobet et al., Elsevier, Amsterdam (1988), p. 13.
- 5) T. Inui, S. Phatanasri, and H. Matsuda, *J. Chem. Soc., Chem. Commun.*, **1990**, 205.
- 6) R. V. Ballmoos and J. B. Higgins, "Collection of Simulated X-Ray Powder Pattern of Zeolites," Butterworth, London (1990).
- 7) N. Ulagappan, S. P. Elangovan, V. Murugesan, and V. Krishnasamy, *Indian J. Chem. Technol.*, in press.
- 8) S. P. Elangovan, V. Krishnasamy, and V. Murugesan, *Indian J. Chem., Sect. A*, **34A**, 469 (1995).
- 9) S. P. Elangovan, V. Krishnasamy, and V. Murugesan, *React. Kinet. Catal. Lett.*, **55**, 153 (1995).
- 10) Ch. Minchev, V. Minkov, V. Penchev, H. Weyda, and H. Lechert, *J. Therm. Anal.*, **37**, 171 (1991).
- 11) Y. Xu, P. J. Maddox, and J. M. Thomas, *Polyhedron*, **8**, 819 (1989).
- 12) A. Stanislaus and L. M. Yeddanapalli, *Can. J. Chem.*, **50**, 61 (1972).
- 13) S. P. Elangovan and V. Krishnasamy, *Indian J. Chem., Sect. A*, **32A**, 1041 (1993).